Redox Driven Swelling of Layer-by-layer Enzyme–Polyelectrolyte Multilayers

ARTICLE *in* LANGMUIR · NOVEMBER 2002

Impact Factor: 4.46 · DOI: 10.1021/la0264419

CITATIONS
46

READS
23

4 AUTHORS:

Erica S Forzani
Arizona State University
56 PUBLICATIONS **1,269** CITATIONS
SEE PROFILE

Manuel Alejo Perez
National University of Cordoba, Argentina
23 PUBLICATIONS **228** CITATIONS
SEE PROFILE

Manuel López Teijelo
National University of Cordoba, Argentina
45 PUBLICATIONS **516** CITATIONS
SEE PROFILE

Ernesto J Calvo
University of Buenos Aires
153 PUBLICATIONS **3,953** CITATIONS
SEE PROFILE

Redox Driven Swelling of Layer-by-layer Enzyme−Polyelectrolyte Multilayers

Erica S. Forzani,[†] Manuel A. Pérez,[‡] Manuel López Teijelo,[‡] and Ernesto J. Calvo*,[†]

INQUIMAE, Departamento de Química Inorgánica, Analítica y Química Física, Facultad de Ciencias Exactas y Naturales, Pabellón 2, Ciudad Universitaria, AR-1428 Buenos Aires, Argentina, and INFIQC, Departamento de Fisicoquímica, Facultad de Ciencias Químicas, Universidad Nacional de Córdoba, Pabellón Argentina, Ciudad Universitaria, AR-5000 Córdoba, Argentina

Received August 20, 2002

Ellipsometric parameters of layer-by-layer self-assembled osmium complex-derivatized poly(allylamine) and glucose oxidase multilayers, $(PAH\text{-}Os)_n(GOx)_n$, were measured at different wavelengths during oxidation−reduction cycles. Data were analyzed using an isotropic single layer model for the enzyme films. The changes in film thickness and refractive index during cyclic voltammetry and potential square wave experiments arise from redox modulation causing film swelling due to the exchange of anions and solvent with the bathing electrolyte. These changes correlate well with the fraction of oxidized PAH-Os(III) in the film.

Introduction

Decher et al.[1−5] introduced a method to build uniform multilayers of polyelectrolytes by stepwise electrostatic adsorption between a charged surface and oppositely charged polymers in solution with molecular level control. Regulation of film thickness and restriction to a monolayer in each adsorption step can be easily achieved by repulsion of a soluble polymer of equal charge. Surface charge reversal operates in every immersion step.[6,7]

The layer-by-layer (LBL) electrostatic self-assembly (ESA) technique has been extended to a wide variety of materials including synthetic polyelectrolytes,[8] proteins,[9] clay minerals,[10] dendrimers,[11] metal[12] and semiconductor colloidal particles,[13] dyes,[14] redox systems,[15] etc. Many applications have been found for the LBL electrostatic self-assembled films: enzyme active films,[16] permselectivity membranes,[17] selective patterning,[18] electrochromism,[19] light-emitting diodes,[8,20] sensors,[21] nonlinear optics,[22] etc.

A number of ordered redox multilayers immobilized on modified electrode surfaces have been described.[23] Laurent and Schlenoff[19b] studied multilayer LBL assemblies of viologen polycation and poly(styrene)sulfonate (PSS) polyanion, where the redox centers through the multilayered structures are electrically addressable via electron hopping between neighboring sites. In these systems, vectorial electron transfer and rectifying effects can be

* To whom correspondence should be addressed. Tel: 005411-4576-3378. E-mail: calvo@qi.fcen.uba.ar.

† INQUIMAE.

‡ INFIQC.

(1) Decher, G. *Science* **1997**, *277*, 1232.

(2) Decher, G.; Hong, J. D.; Schmitt, J. *Thin Solid Films* **1992**, *210/211*, 831.

(3) Decher, G.; Hong, J. D. *Ber. Bunsen-Ges. Phys. Chem.* **1991**, *95*, 1430.

(4) Lvov, Y.; Decher, G.; Sukhorukov, G. *Macromolecules* **1993**, *26*, 5396.

(5) Lvov, Y.; Decher, G.; Mohwald, H. *Langmuir* **1993**, *9*, 481.

(6) Bertrand, P.; Jonas, A.; Laschewsky, A.; Legras, R. *Macromol. Rapid Commun.* **2000**, *21*, 319.

(7) Arys, X.; Jonas, A. M.; Laschewsky, A.; Legras, R. *Supramolecular Polymers*; Ciferi, A., Ed.; Marcel Dekker: New York, 2000; pp 505−563.

(8) Shiratori, S. S.; Rubner, M. F. *Macromolecules* **2000**, *33*, 4213.

(9) Ladam, G.; Gergeli, C.; Seger, B.; Decher, G.; Voegel, J. C.; Schaaf, P.; Cuisinier, F. J. G. *Biomacromolecules* **2000**, *1*, 674.

(10) Kleinfeld, E. R.; Ferguson, G. S. *Science* **1994**, *265*, 370.

(11) (a) Watanabe, S.; Regan, S. L. *J. Am. Chem. Soc.* **1994**, *116*, 8855. (b) Yoon, H. C.; Hong, M. Y.; Kim, H. S. *Anal. Chem.* **2000**, *72*, 4420.

(12) Feldheim, D. L.; Grabar, K. C.; Natan, M. J.; Mallouk, T. C. *J. Am. Chem. Soc.* **1996**, *118*, 7640.

(13) Kotov, N. A.; Dekany, I.; Fendler, J. H. *J. Phys. Chem.* **1995**, *99*, 13065.

(14) Lvov, Y.; Kunitake, T. *J. Am. Chem. Soc.* **1997**, *119*, 2224.

(15) Cheng, L.; Niu, L.; Gong, J.; Dong, S. *Chem. Mater.* **1999**, *11*, 1465.

(16) (a) Onda, M.; Lvov, Y.; Ariga, K.; Kunitake, T. *Biotechnol. Bioeng.* **1996**, *51*, 163. (b) Hodak, J.; Etchenique, R.; Calvo, E. J.; Singhal, K.; Bartlett, P. N. *Langmuir* **1997**, *13*, 2716. (c) Calvo, E. J.; Etchenique, R.; Pietrasanta, L.; Wolosiuk, A.; Danilowicz, C. *Anal. Chem.* **2001**, *73*, 1161. (d) Calvo, E. J.; Battaglini, F.; Danilowicz, C.; Wolosiuk, A.; Otero, M. *Faraday Discuss.* **2000**, *116*, 47. (e) Lvov, Y.; Lu, Z.; Schenkman, J. B.; Zu, X.; Rusling, J. F. *J. Am. Chem. Soc.* **1998**, *120*, 4073. (f) Lvov, Y.; Ariga, K.; Ichinose, I.; Kunitake, T. *J. Am. Chem. Soc.* **1995**, *117*, 6117. (g) Sun, S.; Ho-Si, P. H.; Harrison, D. J. *Langmuir* **1991**, *7*, 727. (h) Mizutani, F.; Sato, Y.; Yabuki, S.; Hirata, Y. *Chem. Lett.* **1996**, 251. (i) Kinnear, K. T.; Monbouquette, H. G. *Langmuir* **1993**, *9*, 2255. (j) Guiomar, A. J.; Guthrie, J. T.; Evans, S. D. *Langmuir* **1999**, *15*, 1198. (k) Onda, M.; Lvov, Y.; Ariga, K.; Kunitake, T. J. *Ferment. Bioeng.* **1996**, *82*, 502. (l) Lvov, Y. *Protein Architecture*; Lvov, Y., Mohwald, H., Eds.; Marcel Dekker: 2000; Chapter 6, p 125. (m) Blonder, R.; Katz, E.; Cohen, Y.; Itzhak, N.; Riklin, A.; Wilner, I. *Anal. Chem.* **1996**, *68*, 3151.

(17) (a) Harris, J. J.; Bruening, M. L. *Langmuir* **2000**, *16*, 2006. (b) Harris, J. J.; Stair, J. L.; Bruening, M. L. *Chem. Mater.* **2000**, *12*, 1941. (c) Stroeve, P.; Vasquez, V.; Coelho, M. A. N.; Rabolt, J. F. *Thin Solid Films* **1996**, *284/285*, 708. (d) Krasermann, L.; Tieke, B. *Langmuir* **2000**, *16*, 287.

(18) Hammond, P. T.; Whitesides, G. M. *Macromolecules* **1995**, *28*, 7569.

(19) (a) Stepp, J.; Schlenoff, J. B. *J. Electrochem. Soc.* **1997**, *144*, L155. (b) Laurent, D.; Schlenoff, J. B. *Langmuir* **1997**, *13*, 1552.

(20) (a) Eckle, M.; Decher, G. *Nano Lett.* **2001**, *1*, 45. (b) Onitsuka, O.; Fou, A. C.; Rubner, M. F. *J. Appl. Phys.* **1996**, *80*, 4067.

(21) Sun, Y.; Zhang, X.; Sun, C.; Wang, B.; Shen, J. *Macromol. Chem. Phys.* **1996**, *197*, 147.

(22) (a) Balasubramamam, S.; Wang, X.; Wang, H. C.; Yang, K.; Kumar, J.; Tripathy, S. K.; Li, L. *Chem. Mater.* **1998**, *10*, 1554. (b) Laschewsky, V. *Thin Solid Films* **1996**, *284*, 334. (c) Lvov, Y.; Yamada, S.; Kunitake, T. *Thin Solid Films* **1997**, *300*, 107.

(23) Anicet, N.; Anne, A.; Moiroux, J.; Savéant, J. M. *J. Am. Chem. Soc.* **1998**, *120*, 7115.

10.1021/la0264419 CCC: $22.00
Published on Web 11/02/2002

achieved. Some interpenetration of the polyions has been confirmed by neutron reflectivity in similar structures.[24,25]

In redox polyelectrolyte multilayers self-assembled using the LBL deposition technique with cationic poly(allylamine) modified with $Os(bpy)_2ClPyCHO$, (PAH-Os) and anionic PSS or poly(vinyl)sulfonate (PVS), the formal redox potential of the Os(II)/Os(III) couple in the polymer film depends on the charge of the outermost layer, the electrolyte concentration, and the pH. At low ionic strength, Donnan permselectivity of anions or cations is apparent and the nature of the ion exclusion from the film is determined by the charge of the topmost layer and the solution pH. At high electrolyte concentration, Donnan breakdown has been observed and the osmium redox potential is close to the value for the redox couple in solution. Exchange of anions and water with the external electrolyte under permselective conditions and salt and water exchange under Donnan breakdown has been observed upon oxidation of the film.

Electroacoustic characterization with the electrochemical quartz crystal microbalance (EQCM) of electrostatically self-assembled films comprised of $(PAH\text{-}Os)_n(GOx)_n$ films both in air and in contact with water during the LBL build up has been reported.[26] These films behave as acoustically thin in the reduced state while for oxidized films, an increase in the acoustic impedance with the number of (PAH-Os)(GOx) bilayers has been observed.[26] From in situ EQCM measurements and measurement of quartz crystal impedance spectrum of films immersed in viscous aqueous electrolyte during the potentiodynamic and potentiostatic experiments, the real (R_S) and imaginary components ($X_{LS} = \omega L_S$) of the quartz complex impedance load were derived. It was shown that the quartz crystal impedance of the composite resonator (film and liquid) increases with the number of deposited layers due to an increase of both the film thickness and the shear modulus.[27] Using a viscoelastic model for the enzyme/polymer film, we have shown that the film acoustic impedance increases with the number of self-assembled layers due to the thickness increase and also to the increase of the shear modulus due to oxidation.[27]

Ellipsometry is a powerful tool to characterize thickness and complex refractive index of thin films by relating the changes of elliptically polarized light measured after incidence on the sample.[28] Ellipsometry has been extensively employed to study the growth of multilayer self-assemblies composed not only of linear[29] and hyperbranched[30] polyelectrolytes but also of anionic enzymes and antibodies.[31] In a previous paper,[32] we have reported ellipsometric measurements carried out on a PAH-Os(II)/GOx self-assembled structure deposited on an 3-mercapto-1-propane-sulfonic acid (MPS)-modified gold surface with a detailed analysis of the optical properties. Both film thickness and film refractive indices were assessed as a function of the number of PAH-Os(II)/GOx pairs of layers at three different wavelengths. Ellipsometry and QCM experiments allowed us to determine the enzyme spatial distribution within the self-assembly as well as LBL apparent density values, concluding that after the fourth (PAH-Os/GOx) bilayer the apparent density is constant with an average value of 1.7 ± 0.2 g cm^{-3}. Additionally, electrochemical experiments allowed us to confirm that a high fraction of the adsorbed PAH-Os is interconnected in the self-assembled structure.[32] The combination of ellipsometry with electrochemistry has allowed the characterization of the dynamics of redox processes in electroactive films, its dependence on the rates of both electron and ion transport in the films, and the morphological changes induced by electrochemical cycling.[28]

In the present paper, we focus on the study of the ellipsometric behavior of PAH-Os/GOx self-assembled films under electrochemical perturbations. We analyze the changes in film thickness and optical properties during oxidation−reduction cycles under both potentiodynamic and potentiostatic conditions. It will be shown that the ellipsometric changes of PAH-Os/GOx thin films (∼300 nm) are related to fast changes in film thickness, occurring simultaneously to the oxidation−reduction of the Os complexes covalently attached to the polymer backbone, due to the exchange of ions and solvent and resulting in film swelling.

Experimental Section

Reagents and Materials. All reagents were used as supplied, and solutions were prepared from Milli Q (Millipore) deionized water. Glucose oxidase (GOx) (EC 1.1.3.4) from *Aspergillus niger* was a gift from MediSense,U.K. The redox polymer $Os(Bpy)_2ClPyCH_2NH$-poly(allylamine), (PAH-Os), was synthesized as previously reported.[33] Polymer solutions were dialyzed against water and used without further purification. Thiol solutions, 20 mM MPS (Aldrich) in 16 mM sulfuric acid (Merck), were prepared before each experiment in order to avoid oxidation in air.

Surface Modification. A 99.99% purity polycrystalline 0.7 cm diameter gold electrode was used as working substrate in the ellipsometric measurements. The surface-cleaning procedure included mechanical polishing, immersion in fresh piranha solution for 10 min, and cycling in deoxygenated 0.5 M H_2SO_4 between −0.2 and 1.5 V vs SCE at 10 V s^{-1}. **Caution: Piranha solution is highly corrosive and reacts violently with organic materials; precautions must be taken at all times when handled.**

We employed the method described by Hodak et al.[16b] to build up LBL supramolecular structures of GOx and PAH-Os, by reverting the surface charge of the topmost layer. First, the gold surface was modified with sulfonate groups by immersion in a 20 mM MPS solution for 30 min followed by rinsing with deionized water. After thiol adsorption, the first PAH-Os layer was formed

(24) Lösche, M.; Schmitt, J.; Decher, G.; Bouwman, W. G.; Kjaer, K. *Macromolecules* **1998**, *31*, 8893.

(25) (a) Schmitt, J.; Grünewald, T.; Decher, G.; Pershan, P. S.; Kjaer, K.; Lösche, M. *Macromolecules* **1993**, *26*, 7058. (b) Lvov, Y.; Haas, H.; Decher, G.; Möhwald, H. *J. Phys. Chem.* **1993**, *97*, 12835. (c) Ferreira, M.; Rubner, M. F. *Macromolecules* **1995**, *28*, 7107.

(26) Calvo, E. J.; Forzani, E. S.; Otero, M. *Anal. Chem.* **2002**, 74, 3281.

(27) Calvo, E. J.; Forzani, E. S.; Otero, M. *J. Electroanal. Chem.* **2002**, in press (JEC 9656).

(28) Gottesfeld, S.; Yeon-Taik, K.; Redondo, A.; In Recent Applications of Ellipsometry and Spectro-ellipsometry in Electrochemical Systems; *Physical Electrochemistry: Principles, Methods and Applications*; Rubinstein, I., Ed.; Marcel Dekker: New York, 1995; Chapter 9.

(29) (a) Keller, S. W.; Hyuk-Nyun, K.; Mallouk, T. E. *J. Am. Chem. Soc.* **1994**, *116*, 8817. (b) Pardo-Yissar, V.; Katz, E.; Lioubashevsky, O.; Willner, I. *Langmuir* **2001**, *17*, 1110. (c) Yang, H. C.; Aoki, K.; Hun-Gi, H.; Sackett, D. D.; Arendt, M. F.; Shueh-Lin, Y.; Bell, C. M.; Mallouk, T. E. *J. Am. Chem. Soc.* **1993**, *115*, 11855. (d) Baur, T. W. Fabrication and Structural Studies of Sequentially Adsorbed Polyelectrolyte Multilayers; Doctoral Thesis, Massachusetts Institute of Technology, 1997. (e) Ginzburg, M.; Galloro, J.; Jäkle, F.; Power-Billard, K. N.; Yang, S.; Sokolov, I.; Catherine Lam, C. N.; Wilhelm Neumann, A.; Manners, I.; Ozin, G. A. *Langmuir* **2000**, *16*, 9609.

(30) Franchina, J. G.; Lackowski, W. M.; Dermody, D. L.; Crooks, R. M.; Bergbreiter, D. E.; Sirkar, K.; Russell, R. J.; Pishko, M. V. *Anal. Chem.* **1999**, *71*, 3133.

(31) (a) Sun, S.; Phuoc-Hoa, H.-S.; Harrison, D. J. *Langmuir* **1991**, *7*, 727. (b) Sirkar, K.; Revzin, A.; Pishko, M. V. *Anal. Chem.* **2000**, *72*, 2930. (c) Arwin, H. *Thin Solid Films* **2000**, *377*−*378*, 48. (d) Spaeth, K.; Brecht, A.; Gauglitz, G. *J. Colloid Interface Sci.* **1997**, *196*, 128.

(32) Forzani, E. S.; Otero, M.; Perez, M. A.; López Teijelo, M.; Calvo, E. J. *Langmuir* **2002**, *18*, 4020−4029.

(33) Danilowicz, C.; Corton, E.; Battaglini, F. *J. Electroanal. Chem.* **1998**, *445*, 89.

by thiol-modified Au substrate immersion in a PAH-Os solution for 5 min. The next and subsequent layers were deposited onto the modified surface by alternated immersions in a 1 μM GOx solution for 10 min and PAH-Os solution (pH 7−8), respectively, and were thoroughly rinsed in deionized water at the end of each adsorption step. As PAH-Os has primary amine groups, it is approximately 10% protonated at the solution pH. No desorption of GOx was observed with the quartz crystal microbalance during rinsing steps.

Ellipsometric Measurements. In ellipsometric measurements, changes in the state of polarization of linearly polarized light due to reflection at a planar surface are detected and the ellipsometric angles Ψ and Δ are determined. These are related to the ellipsometric ratio ρ according to:

$$\rho = \tan(\Psi)\exp(i\Delta) = r_p/r_s \quad (1)$$

where $\tan(\Psi)$ represents the amplitude change in ρ, Δ is the phase difference change, and r_p and r_s are the complex Fresnel reflection coefficients for light polarized parallel and perpendicular to the plane of incidence.[28] The coefficients are dependent on the optical properties and the structure of the interface. Thus, for a multilayer interphase, ρ is a function of the complex refractive index and thickness of each layer as well as the incidence angle (ϕ) and the light wavelength (λ). The complex refractive index of a given medium, $\hat{n}$, is defined as $\hat{n} = n - ik$ where n and k are the refractive index and the extinction coefficient. The simplest model for an ambient-film−substrate system consists of a homogeneous single film sandwiched between the ambient and the substrate. More complicated models can involve film anisotropy or multilayers sandwiched between the substrate and the ambient.[28] In the present paper, the model used to describe the ellipsometric data considers the LBL self-assembled films as a single layer of isotropic optical properties. In this case, the experimental data were fitted using the Simplex method to minimize the error function:

$$\chi(n_f, k_f, d_1, d_2, ..., d_M) = \frac{1}{M}\sum_{i=1}^{M}[(\Psi_i - \Psi_i^{calcd})^2 + (\Delta_i - \Delta_i^{calcd})^2]^{1/2} \quad (2)$$

where the superscript "calcd" denotes the values calculated from the model.[34]

A Rudolf Research rotating analyzer automatic ellipsometer (vertical type, 2000FT model), equipped with a 75 W tungsten lamp as light source and filters (632.8, 546.1, and 405.0 nm), was used. All measurements were performed at an angle of incidence of 70.00°. The gold electrode was mounted horizontally in a PTFE holder and aligned before each experiment. All experiments were carried out taking care of the system alignment and avoiding any variations of the electrode position. Ellipsometric parameters (Ψ and Δ) were collected in continuous mode for freshly built up films (unless otherwise stated). As GOx is a photosensitive molecule, all of the optical measurements were performed in a dark room to avoid possible photodecomposition, which can affect the structure of the protein.[35] Furthermore, the 546.1 nm filter was mounted before the polarizer, allowing only this selected wavelength to reach the modified gold surface during the adsorption, washing, and drying steps.

Electrochemical Setup. A standard three electrode electrochemical cell fitted with two glass windows was employed. A gold electrode (diameter ~ 0.7 cm) was used as the working electrode. The reference electrode was an SCE, and all potentials herein are quoted with respect to this electrode. A platinum plate (diameter ~ 2 cm) was employed as the counter electrode.

Results and Discussion

Cyclic Voltammetry. Figure 1 depicts a typical cyclic voltammogram for a self-assembled $(PAH\text{-}Os)_7(GOx)_7$ multilayer on a thiolated gold surface. A peak separation

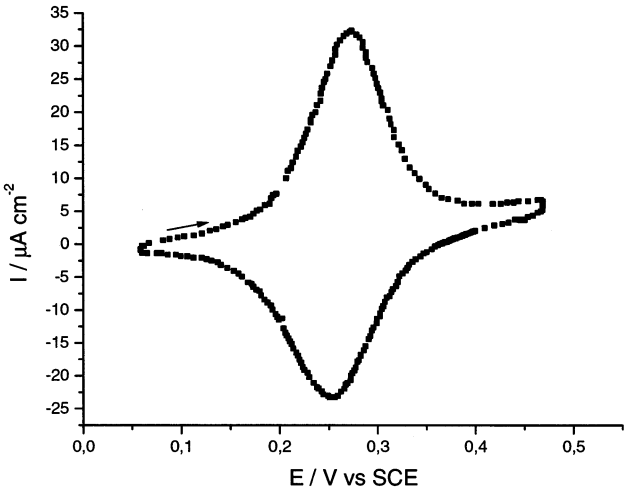

Figure 1. Cyclic voltammogram of a $(PAH\text{-}Os)_7/(GOx)_7$ self-assembled film obtained at 5 mV s^{-1} in 0.12 M KNO_3, 0.1 M Tris buffer (pH 7.2).

of less than 12 mV and a full width at half-height (fwhh) close to the theoretical value for an ideal Nernstian surface layer for a one electron transfer process (90.6 mV) are obtained. The anodic and cathodic peak currents increase proportionally to the potential scan rate (v), indicating that all redox sites in the film can be oxidized in the time scale of the experiment at relatively high sweep rates of 1 V s^{-1} (not shown), i.e., $vF/RT \leq 40$ s^{-1}. The integrated charge also increases with the number of added LBL self-assembled layers. Charge propagation through the consecutive PAH-Os/GOx layers takes place by electron hopping between adjacent osmium redox centers in the polymer in a diffusion-like process with $D_e \approx 10^{-9}$ cm^2 s^{-1}.[36]

From experimental evidence with the EQCM, we found a mass increase during the oxidation of the Os(II) to Os(III) sites in the $Os(bpy)_2ClPyCHNH$-modified polymer.[27] This was interpreted in terms of the entrance of anions and solvent into the polymer thin film to compensate for the electrical charge and swelling of the film. Therefore, it is to be expected that the film thickness increases during film oxidation.

Figure 2 shows the $\Psi-\Delta$ response of LBL self-assembled films during a potentiodynamic cycling at 5 mV s^{-1} for films formed after a different number (indicated by numerals) of enzyme−polymer adsorption steps. The difference between the optical response corresponding to the oxidized and reduced states increases with the number of bilayers, indicating that the optical properties of the film are dependent on the oxidation state of the Os sites. The $\Psi-\Delta$ responses of the oxidized and reduced states for an increasing number of adsorption steps (increase of film thickness) have allowed us to determine the dependence of the optical properties on the oxidation state of the Os sites in the film as well as the corresponding thickness values. The best fit obtained for the two different data sets by using the single layer model yield $\hat{n} = 1.454 - 0.003i$ for the oxidized state and $\hat{n} = 1.466 - 0.006i$ for the reduced film at 546.1 nm, indicating that the optical properties depend on the redox state of the multilayer film. Also, the thickness values obtained show an increase upon film electrooxidation (see below).

To obtain the dependence of optical properties and thickness with electrode potential, the Ψ and Δ depen-

(34) De Smet, D. J.; Ord, J. L. *J. Electrochem. Soc.* **1989**, *136*, 2841.
(35) Szucs, A.; Hitchens, G. D.; Bockris, J. O'M. *J. Electrochem. Soc.* **1989**, *136*, 3748.
(36) Calvo, E. J.; Danilowicz, C.; Wolosiuk, A. *J. Am. Chem. Soc.* **2002**, *124*, 2452.

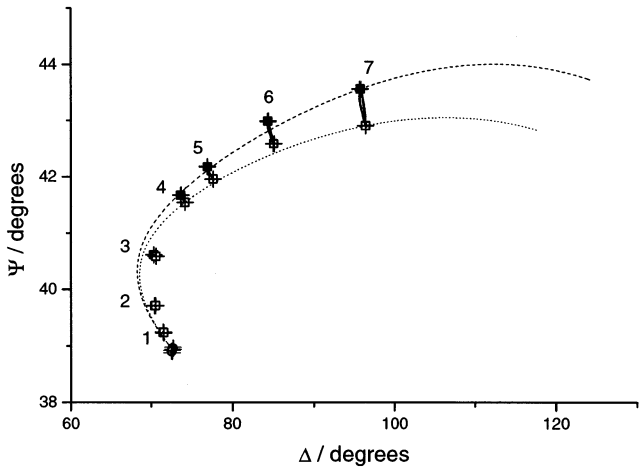

Figure 2. Ψ−Δ response of PAH-Os/GOx self-assembled multilayer films of different thickness during the potentiodynamic cycling at 5 mV s^{-1} between 0.006 and 0.046 V in 0.10 M KNO_3, 0.1 M Tris buffer (pH 7.5). Numerals indicate the number of previous PAH-Os/GOx adsoption steps. Ψ−Δ values of the film in its fully reduced (□) and fully oxidized (■) states are also indicated. The dashed and dotted lines correspond to the best fitting curves with the single layer model for both the oxidized and the reduced states (λ = 546.1 nm).

dence on potential for a seven enzyme−redox polymer layer during a potentiodynamic oxidation/reduction cycle at 5 mV s^{-1} was measured (Figure 3). A wavelength value of 632.8 nm was chosen here to perform the optical measurement since there is a null absorption of both components of the multilayer, i.e., glucose oxidase or the osmium bipyridyl complex.[32] For this film, the oxidation of Os(II) to Os(III) results in an increase of Ψ and a decrease of Δ. Both the Ψ-E and Δ-E responses show a very slight hysteresis between the forward and the reverse potential sweeps, indicating the existence of a slight optical irreversibility between the film oxidation and the reduction processes. This indicates that the charge/discharge process gives rise to regions with different optical properties; hence, the film should be regarded, at least, as a bilayer. On the other hand, the small difference found in the optical properties for the oxidized and reduced states indicates that the effect of the slight optical irreversibility should be negligible, at least in the time scale of the experiment, as expected for a film with a reversible redox thin layer voltammetric response (Figure 1). Therefore, during the charge/discharge process, the enzyme−redox polymer film can be considered to be a very good approximation, as a layer with homogeneous optical properties. In addition, because the film is transparent (k = 0) at λ = 632.8 nm,[32] the optical changes during the charge/discharge process should be associated with changes in the refractive index and thickness of the film. Consequently, the Ψ−Δ response obtained during the film oxidation/reduction process was analyzed in terms of the single layer model. Theoretical curves were simulated for different refractive index values comprised between those for the oxidized and reduced states. The refractive index and thickness values at different potentials were obtained from the crossing point of each curve and the charge/discharge ellipsometric curve.

Figure 4 shows the dependence of the resulting thickness and refractive index with potential obtained for a self-assembled multilayer film, during potential cycling at 5 mV s^{-1}. It is worthwhile noting that the film thickness increases by some 10% from the fully reduced to the fully oxidized state, while a decrease in the refractive index of only 2.9% is apparent. These results are consistent with EQCM evidence,[27] i.e., the expected film swelling produced

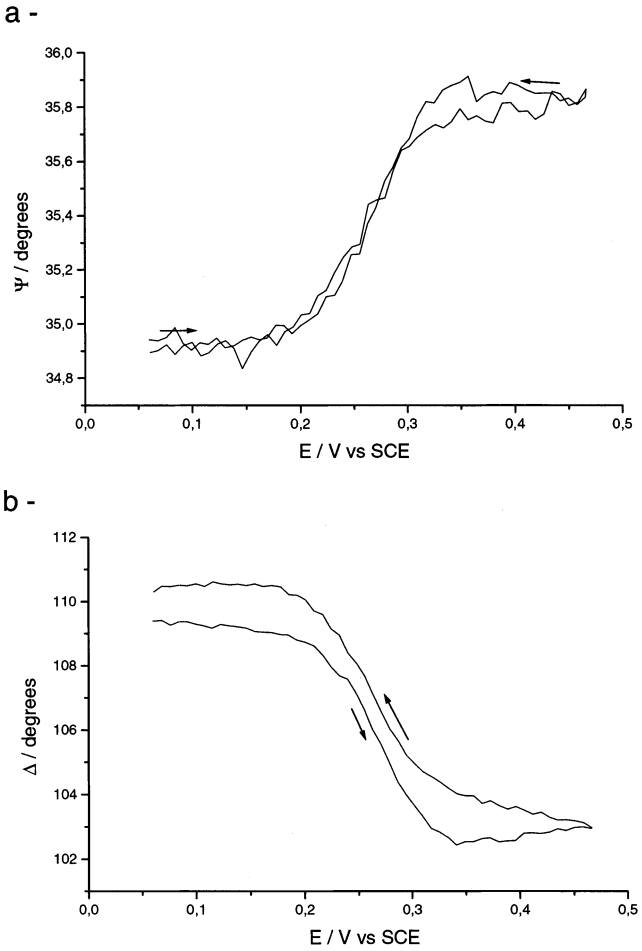

Figure 3. (a) Ψ-E and (b) Δ-E dependencies of a $(PAH\text{-}Os)_7/(GOx)_7$ multilayer film during potentiodynamic cycling at 5 mV s^{-1} in 0.12 M KNO_3, 0.1 M Tris buffer (pH 7.2) (λ = 632.8 nm). The experiment was performed on a fresh system self-assembled at the open circuit potential and at a constant ionic strength.

by the entrance of anions and solvent coming from the bathing electrolyte and the increase of water content (n_{water} = 1.33) within the film. The small change obtained in the refractive index corroborates the assumption of considering the film as a layer with homogeneous optical properties. On the other hand, because the optical response does not change after several successive potential cycles (not shown), the films are stable in both the oxidized and the reduced states.

From gravimetric[27] and the present ellipsometric results, the oxidation of Os(II) sites in the redox self-assembled $(PAH\text{-}Os)_n(GOx)_n$ film can be represented as

$$[PAH-Os(II)]_{polym} + yH_2O + X^- \rightarrow [PAH-Os(III)\cdot X^-\cdot yH_2O]_{polym} + e^- \quad (3)$$

where X^- represents an anion in solution that is incorporated into the polymer film during oxidation to compensate for the change in electrical charge. Furthermore, anion exchange during oxidation of related films is supported by the negative slope of E_{peak} vs ln c plots due to Donnan permselectivity,[37] with c as the ionic concentration of KNO_3 electrolyte.

Experimental semiquantitative evidence of charge-to-mass ratio from the EQCM experiments has shown that

(37) Calvo, E. J.; Wolosiuk, A. *J. Am. Chem. Soc.* **2002**, *124*, 8490.

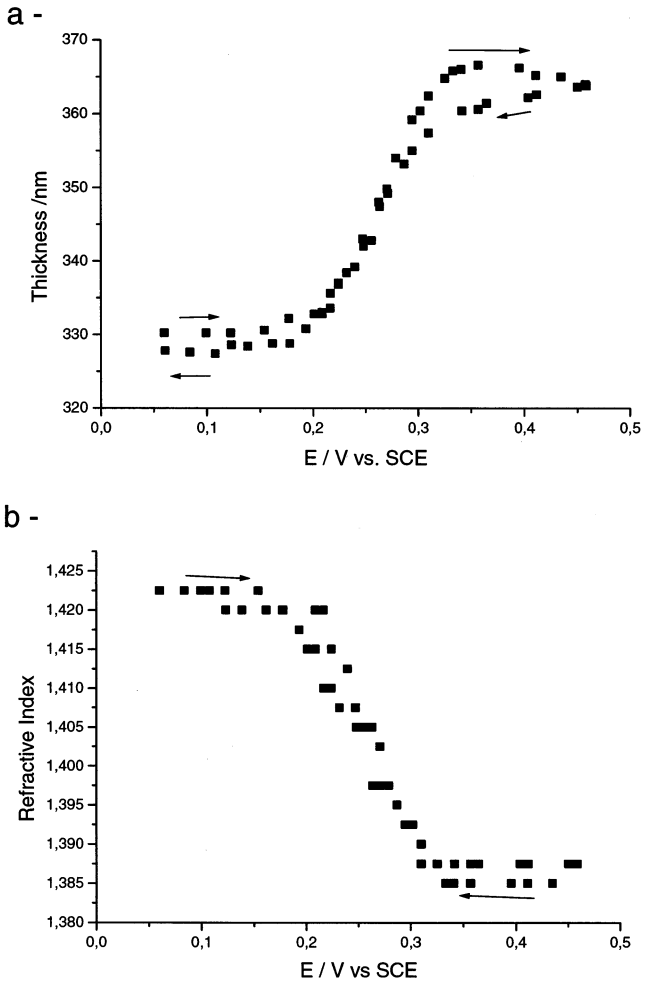

Figure 4. Plots of (a) d_f-E and (b) n_f-E dependencies obtained for a (PAH-Os)$_7$/(GOx)$_7$ multilayer film under potentiodynamic conditions ($v = 5$ mV s^{-1}), at $\lambda = 632.8$ nm. Optical properties obtained by simulation of $\Psi-\Delta$ values similar to those shown in Figure 3 with an isotropic single layer model on thiolated gold ($n = 0.767$, $k = 2.540$), assuming k (632.8 nm) = 0.000.

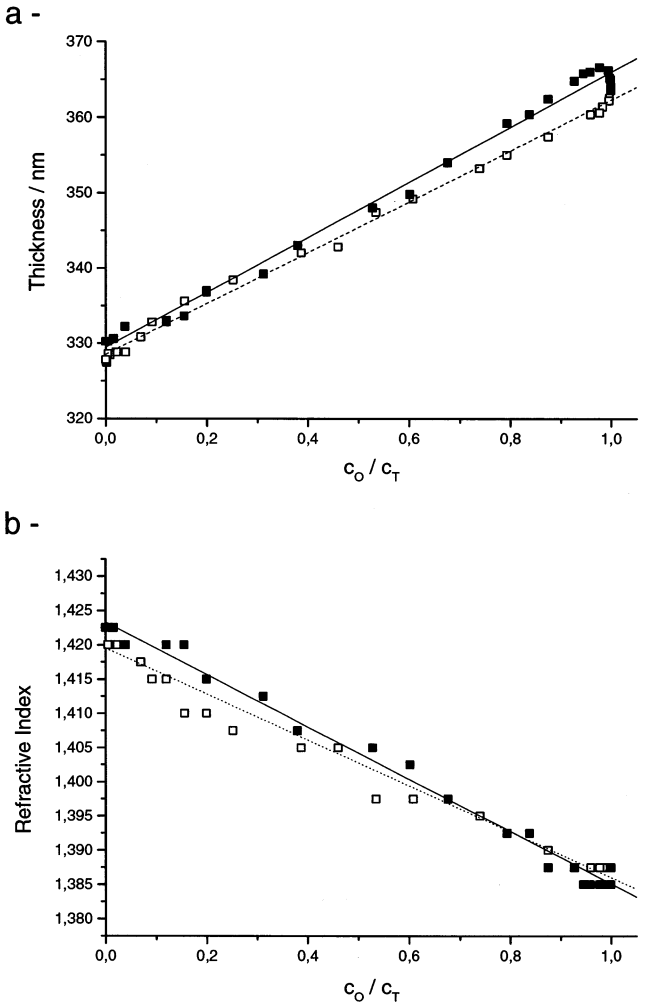

Figure 5. Plots of (a) d_f-(c_O/c_T) and (b) n_f-(c_O/c_T) dependencies obtained for a (PAH-Os)$_7$/(GOx)$_7$ multilayer film under potentiodynamic conditions ($v = 5$ mV s^{-1}).

a large amount of water enters into the film per Os(III) site, which would result in an important film thickness increase for the swollen polymer (see below). Careful analysis of eq 3 indicates that one would expect a correlation between the thickness increase and the fraction of oxidized redox sites. The Nernstian behavior of (PAH-Os)$_n$(GOx)$_n$ enzyme−polyelectrolyte thin films predicts that the fraction of oxidized osmium sites in the film depends on the electrode potential as

$$\frac{Q_{ox}}{Q_T} = \frac{c_O}{c_T} = \frac{\exp\left[\frac{nF}{RT}(E - E_{1/2})\right]}{1 + \exp\left[\frac{nF}{RT}(E - E_{1/2})\right]} \qquad (4)$$

where Q_T is the total charge for the fully oxidized film, c_O = [PAH−Os(III)·X$^-$·yH$_2$O] represents the concentration of Os(III), c_T is the total concentration of osmium sites in the film, and $E_{1/2}$ is the half wave redox potential of the osmium polymer in the multilayer ($E_{1/2} = 0.26$ V vs SCE).

Figure 5 shows a linear dependence for both the film thickness and the refractive index on the fraction of Os(III) for a (PAH−Os)$_7$(GOx)$_7$ multilayer film. This is strong evidence that the amount of water that enters into the film per mole of Os(III) formed is almost constant; hence, the film volume increase per Faraday of electrical charge is also almost constant. The film thickness is thus given by

$$d_f = d_f(\mathrm{Os(II)}) + \frac{C_O}{C_T}\Delta d_f \qquad (5)$$

where d_f(Os(II)) represents the film thickness of the totally reduced film and Δd_f is the maximum thickness change. The linear decrease in refractive index is also consistent with the ingress of water into the film.

For a quantitative assessment of the charge-to-mass ratio resulting from the oxidation of the redox self-assembled (PAH−Os)$_7$(GOx)$_7$ multilayer, $\Delta m/\Delta Q$, the integrated electrical charge during a voltammetric cycle and the simultaneous mass change should be taken into account. In the general case, the change in mass is the sum of the mass due to the ions (anions and cations), the mass due to salt (if Donnan breakdown occurs[37]), and the mass due to solvent exchange during film oxidation and reduction. For the enzyme films reported here, we have found that anion exchange occurs under Donnan perm-selectivity; therefore, only anion and solvent contribute to the mass change during redox driven swelling of the film.

The mass increase was obtained from the gravimetric measurement with the quartz crystal microbalance from the resonant frequency shift during film oxidation with the Sauerbrey equation.[27] However, during (PAH−Os)$_7$-

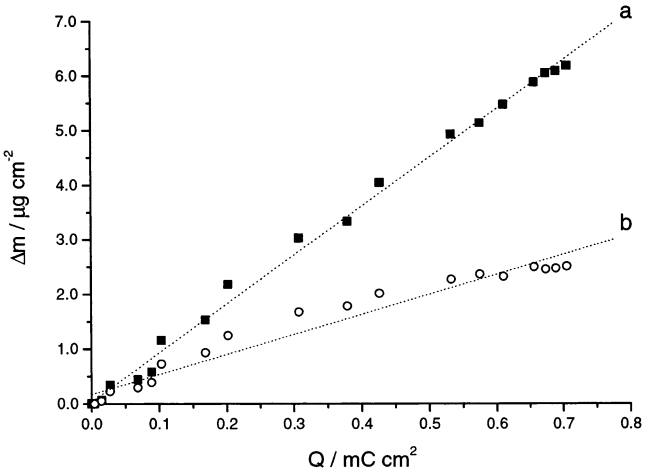

Figure 6. Plots of mass to charge dependence for the oxidation of a $(PAH\text{-}Os)_7/(GOx)_7$ multilayer film under potentiodynamic conditions ($v = 5$ mV s^{-1}). (a) Mass obtained from ellipsometric thickness and film density and (b) ellipsometric mass calculated with eq 6.

$(GOx)_7$ film oxidation, the EQCM measures a mass in defect with respect to the value expected from thickness change alone assuming a constant density of 1.7 g cm^{-3} for the reduced film.[27] This is due to the attenuation of the acoustic wave in the viscoelastic film and viscous electrolyte solution; the shear wave in the film is attenuated more the more oxidized is the film.

The total mass increase from the reduced to the fully oxidized film was found to be 4.3 μg cm^{-2} (see Supporting Information) and the total redox charge 0.7 mC cm^{-2}, which yielded an exchange of 595 g mol^{-1}. Because of the viscoelastic coupling,[27] it is expected that the actual exchanged mass should be larger than this value.

A lower limit, on the other hand, was assessed from the ellipsometric areal mass density, Δm_e, obtained from the optical film thickness, d_f, and film refractive index, n_f, through the de Feijter equation,[38] which has been widely employed for protein films:

$$\Delta m_e = d_f \frac{n_f - n_o}{\partial n/\partial c} \qquad (6)$$

where n_o is the electrolyte refractive index and $\partial n/\partial c$ is the refractive index increment of the exchanged solution with concentration. For KNO_3 solutions in the concentration range of 0−0.27 g mL^{-1}, we have obtained a linear relationship with $\partial n/\partial c = 0.089$ cm^3 g^{-1} (see Supporting Information). Because water molecules and ions within the film are not polarized in the visible spectral region, the low optical contrast between film and solvent prevents an accurate measurement of the most hydrated external regions of the enzyme−polymer film[32] while they are sensed by the quartz crystal microbalance. It should be noticed that the de Feijter equation fails to account for mass increase when the main exchanged species is water since in that case there is no appreciable increment in the refractive index.

The resulting ellipsometric mass data are plotted in Figure 6 as a function of the electrical charge for the oxidation of Os(II) and yields 340 g mol^{-1}. Note that even this lower limit of mass increase per Faraday of charge consumed in oxidizing the Os(II) sites is much higher than the molar mass of any of the anions in solution; therefore,

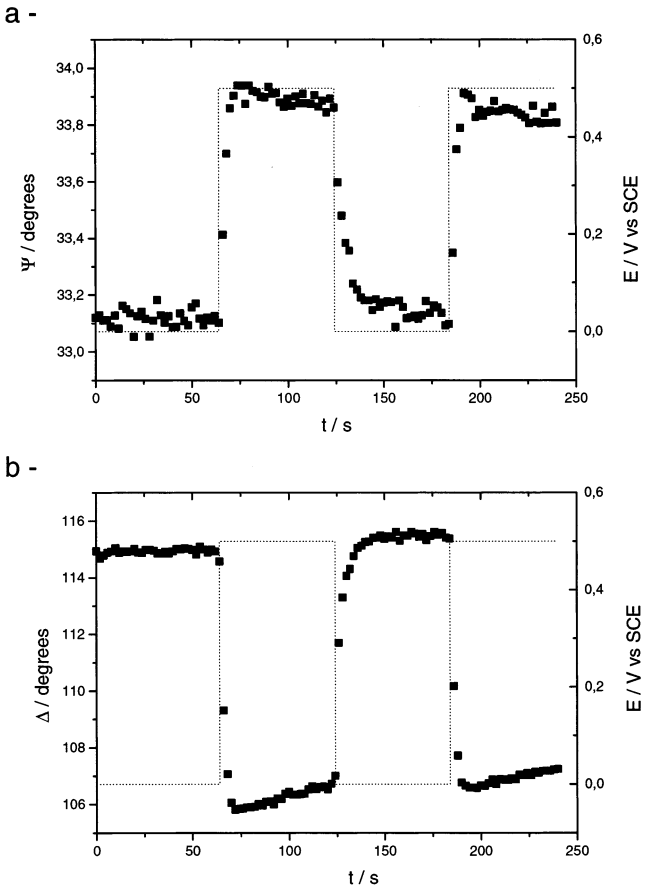

Figure 7. Effect of 0.000 and 0.500 V alternated potential steps on (a) Ψ and (b) Δ values obtained at 632.8 nm for a $(PAH\text{-}Os)_7/(GOx)_7$ multilayer in 0.12 M KNO_3, 0.1 M Tris buffer (pH 7.5). The experiment was performed on a fresh system self-assembled at the open circuit potential and at a constant ionic strength. Adsorption steps of PAH-Os layers by a 5 min immersion in a 0.16% P/V solution and of GOx layers by a 10 min immersion in a 1 μM solution.

one concludes that most of the mass increase is due to the incorporation of water into the oxidized film producing swelling.

Another approximation to the exchanged mass is to consider the film ellipsometric thickness increase, $\Delta m = \rho_f \Delta d_f$ at constant film density, ρ_f, during the film redox driven swelling. Although the mass increase may result in both changes of film thickness, d_f, and changes of film density, ρ_f, no independent evidences to separate both thickness and density contributions during film swelling have been found in this study. However, from the gravimetric and ellipsometric results, a constant mass and volume increase per mole of Os(II) sites has been observed. Furthermore, less than 3% variation in the film refractive index suggests a rather constant film density during swelling; then, the average reduced film density 1.7 ± 0.2 g cm^{-3} from gravimetric and ellipsometric measurements beyond the fourth enzyme−polymer bilayer in the reduced state[32] can be used to estimate the mass increase during swelling. Figure 6 shows a linear dependence of the mass increase (from ellipsometric thickness increase) with osmium oxidation charge with a slope of 8.56 mg C^{-1} from which 826 g of anions and water per mole of Os(III) was obtained. This upper limit of mass increase per Faraday of charge consumed in oxidizing the Os(II) sites is also much higher than the molar mass of any of the anions present in solution; thus, we conclude that most of the mass increase is due to the incorporation of water into the oxidized film, which results in swelling

(38) Hahn Berg, I. C.; Muller, D.; Arnebrant, T.; Halmsten, M. *Langmuir* **2001**, *17*, 1641−1652.

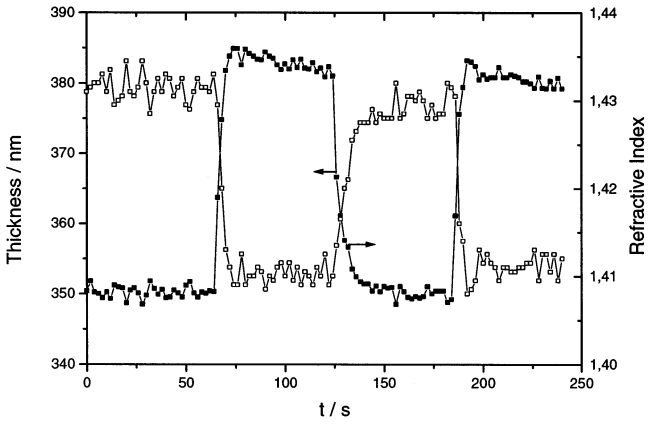

Figure 8. Effect of 0.000 and 0.500 V alternated potential steps on (■) thickness and (□) refractive index of a $(PAH\text{-}Os)_7/(GOx)_7$ multilayer. Optical properties obtained by simulation of $\Psi-\Delta$ values similar to those shown in Figure 7 with an isotropic single layer model on thiolated gold ($n = 0.864$, $k = 2.461$), assuming k (632.8 nm) = 0.000.

as has been observed during the oxidation of similar hydrogels formed with the same components, PAH-Os and GOx.[39]

Chonoamperometry. In the previous discussion, we have presented results at a low sweep rate (5 mV s^{-1}). Therefore, if no concentration gradients in the direction perpendicular to the electrode are established, the osmium redox film can be considered as homogeneous. We next examined the change of the ellipsometric parameters with time as the $(PAH\text{-}Os)_7(GOx)_7$ self-assembled multilayer films are oxidized and reduced under a potential square wave perturbation. Figure 7 depicts the time dependence of Ψ (a) and Δ (b) during oxidation and reduction. A very fast transition between two well-defined states is observed in both cases with the same trend as seen in Figure 3 for cyclic voltammetry experiments. However, note that a faster response is seen for the switch on transient (Os(II) to Os(III) step). The changes in film thickness and refractive index at 632.8 nm obtained as it was described before from the ellipsometric angles Ψ and Δ are shown in Figure 8 as a function of time. The fast thickness and refractive index changes between the fully oxidized and the fully reduced states follow the same trend as in cyclic voltammetry experiments, which suggests that both solvent and ion population changes are fast. While polymer-modified electrodes usually show a slow relaxation upon redox switching, the fast process observed for oxidation−reduction of the self-assembled $(PAH\text{-}Os)_7(GOx)_7$ multilayer film (~300 nm thick) could be associated to the small thickness of the film. For a hydrogel of similar composition, we have found an electron hopping diffusion coefficient of 10^{-9} to 10^{-10} cm^2 s^{-1}, [38] so taking a conservative value of 10^{-10} cm^2 s^{-1}, full oxidation of a 300 nm film will be achieved in a few milliseconds. The time scale of our transients in Figure 8 may be due to exchange of solvent in a slower time scale than the anion and electrons.[40]

Conclusions

The optical response of PAH-Os/GOx self-assembled multilayers was determined by in situ ellipsometry under potential-controlled conditions and fitted using an isotropic single layer model. Optical reversibility was observed during film oxidation−reduction cycles performed both potentiodynamically and potentiostatically. Typically, a 10% thickness increase and 3% refractive index decrease were observed when PAH-Os/GOx films were completely oxidized, which was associated to film swelling produced by the entrance of anions and water. The changes in thickness and refractive index are proportional to the fraction of oxidized osmium centers in the film and therefore can be modulated by the redox charge injected electrochemically into the film.

Acknowledgment. Financial support from the University of Buenos Aires, University of Córdoba, CONICET, ANPCyT, and ACC are gratefully acknowledged. E.F. also thanks CONICET for a postdoctoral fellowship. E.J.C. acknowledges a Guggenheim Fellowship 2000/2001.

Supporting Information Available: Plot of oxidation of $(PAH\text{-}Os)_7(GOx)_7$, plot of R_S vs X_{LS}, and plot of refractive index vs electrolyte concentration. This material is available free of charge via the Internet at http://pubs.acs.org.

LA0264419

(39) Etchenique, R.; Calvo, E. J. *J. Phys. Chem. B* **1999**, *103*, 8944.

(40) Hillman, A. R. *Solid State Ionics* **1997**, *94*, 151.